JOC Article
pubs.acs.org/joc

OsO_4-Mediated Dihydroxylation of *meso*-Tetraphenylporphyrin *N*-Oxide and Transformation of the Resulting Diolchlorin *N*-Oxide Regioisomers

Subhadeep Banerjee,[†] Matthias Zeller,[‡] and Christian Brückner*,[†]

[†]*Department of Chemistry, University of Connecticut, Unit 3060, Storrs, Connecticut 06269-3060 and* [‡]*Department of Chemistry, Youngstown State University, One University Plaza, Youngstown, Ohio 44555-3663*

c.bruckner@uconn.edu

Received November 12, 2009

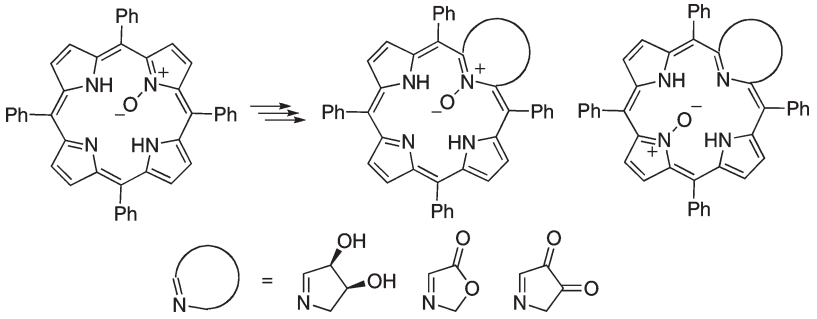

The OsO_4-mediated dihydroxylation of *meso*-tetraphenylporphyrin *N*-oxide yields two regioisomeric chlorin *N*-oxides. These chlorin *N*-oxides can be manipulated to provide pairs of regioisomers of pyrrole-modified porphyrin *N*-oxides. The UV−vis absorption and fluorescence emission spectra of the neutral and protonated regioisomers are distinct from each other, and generally different from the parent chromophore. The outcome of diol oxidation reactions of some *N*-oxide diolchlorins varies from the corresponding reactions of the parent diolchlorins. The crystal structure of a free base porpholactone *N*-oxide carrying the *N*-oxide on the oxazolone moiety is reported.

Introduction

Octaethylporphyrin (OEP) *N*-oxide or *meso*-tetraarylporphyrin *N*-oxides (such as **1**, Scheme 1), and their metal complexes, have been known for about 30 years.[1−6] Their biological significance derives from the presumed involvement of porphyrin *N*-oxide Fe(III) complexes in heme degradation and P-450 suicide reactions.[3,7−9] Their photophysical properties are, largely on account of their nonplanar conformation, significantly different from those of free base porphyrins. Thus, the in-depth investigation of porphyrinoid *N*-oxides might provide chromophores with photophysical properties that are more suitable for a given technical or biomedical application than the parent chromophore.

We recently reported an improved synthesis of porphyrin *N*-oxides by oxidation of the corresponding free base porphyrin in which, instead of using hypofluorous acid or organic peracids (peracetic, permaleic acid),[2,3,10] we used a

*To whom correspondence should be addressed. Fax: (+1) 860 486-2981. Tel: (+1) 860 486-2743.

(1) Bonnett, R.; Ridge, R. J.; Appelman, E. H. *J. Chem. Soc., Chem. Commun.* **1978**, 310–11.

(2) Andrews, L. E.; Bonnett, R.; Ridge, R. J.; Appelman, E. H. *J. Chem. Soc., Perkin Trans. 1* **1983**, 103–107.

(3) Balch, A. L.; Chan, Y. W.; Olmstead, M.; Renner, M. W. *J. Am. Chem. Soc.* **1985**, *107*, 2393–2398.

(4) Balch, A. L.; Chan, Y.-W.; Olmstead, M. M. *J. Am. Chem. Soc.* **1985**, *107*, 6510–6514.

(5) Yang, F.-A.; Cho, K.-Y.; Chen, J.-H.; Wang, S.-S.; Tung, J.-Y.; Hsieh, H.-Y.; Liao, F.-L.; Lee, G.-H.; Hwang, L.-P.; Elango, S. *Polyhedron* **2004**, *25*, 2207–2214.

(6) Yang, F.-A.; Guo, C.-W.; Chen, Y.-J.; Chen, J.-H.; Wang, S.-S.; Tung, J.-Y.; Hwang, L.-P.; Elango, S. *Inorg. Chem.* **2007**, *46*, 578–585.

(7) Mizutani, Y.; Watanabe, Y.; Kitagawa, T. *J. Am. Chem. Soc.* **1994**, *116*, 3439–3441.

(8) Rachlewicz, K.; Latos-Grazynski, L. *Inorg. Chem.* **1996**, *35*, 1136–47.

(9) (a) Groves, J. T.; Watanabe, Y. *J. Am. Chem. Soc.* **1986**, *108*, 7836–7837. (b) Groves, J. T.; Watanabe, Y. *J. Am. Chem. Soc.* **1988**, *110*, 8443–8452.

(10) For an alterative, non-general photochemical pathway toward the Ti=O complex of a porphyrin *N*-oxide, see: Hoshino, M.; Yamamoto, K.; Lillis, J. P.; Chijimatsu, T.; Uzawa, J. *Inorg. Chem.* **1993**, *32*, 5002–5003.

DOI: 10.1021/jo9024286 Published on Web 01/12/2010

SCHEME 1. Preparation of Four Pairs of Porphyrin- and Chlorin *N*-Oxide Regioisomers

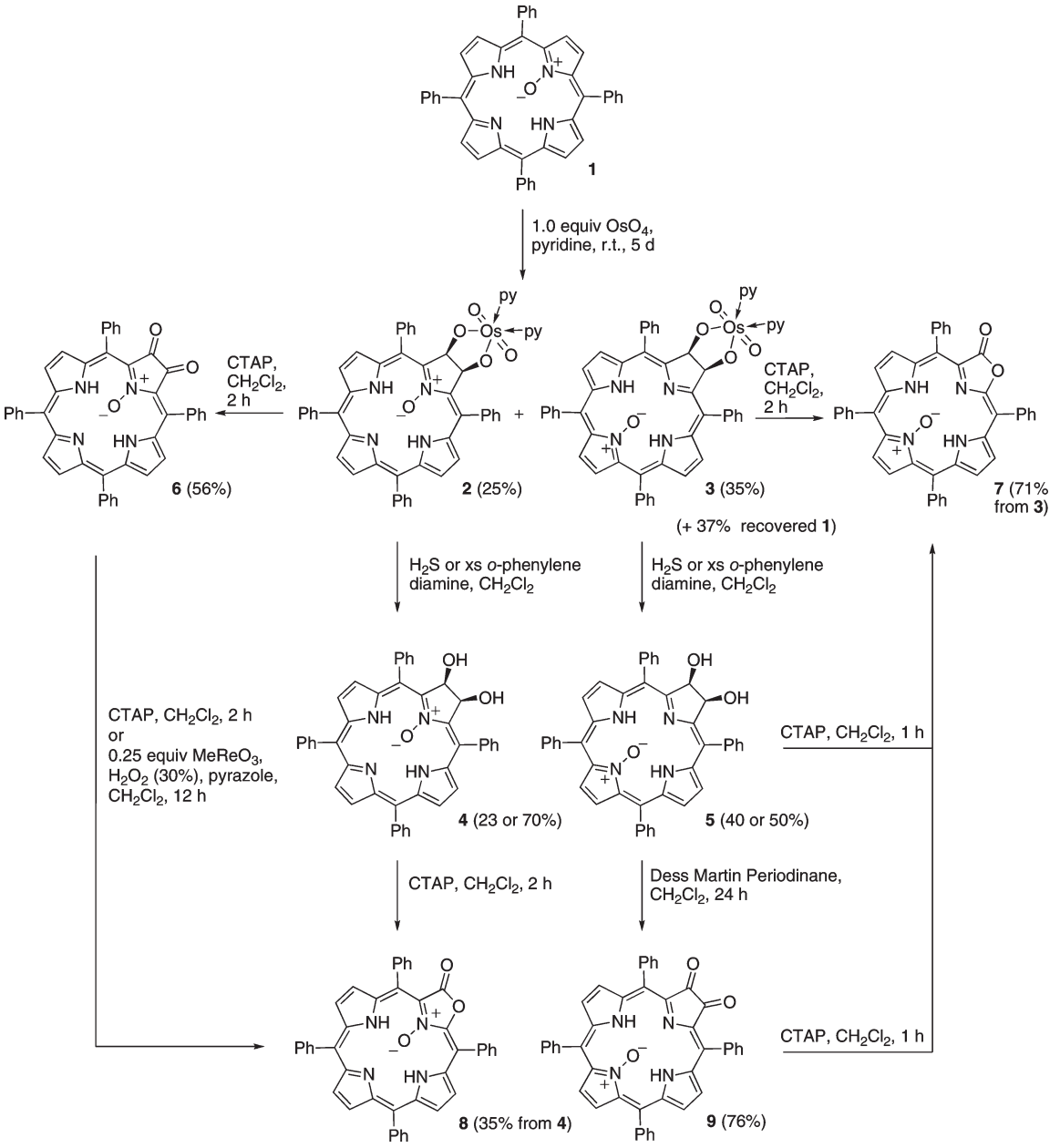

methyltrioxorhenium (MTO)-catalyzed H_2O_2 oxidation in the presence of pyrazole.[11] The yields of this reaction vary with the porphyrin and range from moderate (14% for *meso*-tetrapentafluorophenylporphyrin) to acceptable (70% for *meso*-tetraphenylporphyrin), whereby the low yields are due to low conversions, and most of the starting materials can be recovered. Importantly, this *N*-oxidation methodology was mild enough to allow the preparation of the hitherto unknown chlorin *N*-oxides, *meso*-tetraphenylporpholactone *N*-oxide, and thiaporphyrin *S*-oxides.

Little is known about the chemical reactivity of the porphyrin *N*-oxides. They can be metalated.[6,14] OEP *N*-oxide, in its free base or Ni(II) complex form, can be rearranged into a β-oxochlorin or its metal complex, respectively.[2,12] Also, the Fe(III) complex of *meso*-tetramesitylporphyrin-*N*-oxide, upon treatment with TFA, converted to an unusual ring-oxidized Fe(III) porphyrin complex.[13]

We are interested in the β,β'-bond modification of porphyrins and the study of the reactivity and photophysical properties of the resulting pyrrole-modified porphyrins. As an entry point into the manipulation of the pyrrole moieties, we have largely relied on the stoichiometric OsO_4-mediated dihydroxylation of octaethylporphyrin and

(11) Banerjee, S.; Zeller, M.; Brückner, C. *J. Org. Chem.* **2009**, *74*, 4283–4288.

(12) Balch, A. L.; Chan, Y. W. *Inorg. Chim. Acta* **1986**, *115*, L45–L46.

(13) Tsurumaki, H.; Watanabe, Y.; Morishima, I. *J. Am. Chem. Soc.* **1993**, *115*, 11784–11788.

(14) (a) Tsurumaki, H.; Watanabe, Y.; Morishima, I. *Inorg. Chem.* **1994**, *33*, 4186–4188. (b) Arasasingham, R. D.; Balch, A. L.; Olmstead, M. M.; Renner, M. W. *Inorg. Chem.* **1987**, *26*, 3562–3568.

meso-tetraarylporphyrins.[15−20] Having now ready access to *meso*-tetraphenylporphyrin *N*-oxide (**1**),[11] this prompted us to investigate whether this chromophore is also susceptible to an OsO_4-mediated dihydroxylation. And if so, how does this dihydroxylation vary when compared to the dihydroxylation of the corresponding *meso*-tetraphenylporphyrin or -chlorin? For instance, will regioisomers (dihydroxylation on a pyrrole or an *N*-oxidized pyrrole) be formed or will the reaction be regioselective, as observed for the *N*-oxidation of a chlorin? Furthermore, are the *N*-oxidized diolchlorins susceptible to diol functional group interconversions, and if so, will their course be different from those of the non-*N*-oxidized analogues?

We describe here the results of this study. In short, many of the questions posed can be answered in the affirmative. This study also provides access to a number of intriguing porphyrinoid *N*-oxide chromophores that are inaccessible by direct *N*-oxidation of the corresponding macrocycle or along other known synthetic pathways.

Results and Discussion

Dihydroxylation of *meso*-Tetraphenylporphyrin *N*-Oxide. Parallel to the dihydroxylation of *meso*-tetraphenylporphyrin,[16] the reaction of *meso*-tetraphenylporphyrin *N*-oxide (**1**) with 1.0 equiv of OsO_4 in pyridine at ambient temperature requires 5 days until no further change of the reaction mixture could be detected by TLC and UV−vis spectroscopy. Upon chromatographic separation, we obtained a 1:1.3 mixture of two products, **2** and **3**, in yields of 25% and 30−35%, respectively (37% of the starting material was recovered) (Scheme 1). Since the higher polarity product possessed identical UV−vis absorption spectra as a previously reported 2,3-dimethoxychlorin *N*-oxide in which *N*-oxidation had taken place at the pyrrole opposite of the diolpyrrolidine moiety,[11] we assigned it chlorin osmate ester bispyridine complex structure **3** and the lower polarity fraction tentatively the isomeric structure **2**. As we will detail below, we were able to unambiguously confirm this assignment. The reaction is, as compared to the reaction of *meso*-tetraphenylporphyrin with OsO_4 under similar conditions,[16] neither significantly inhibited nor accelerated. Furthermore, the near 1:1 ratio of the two products indicates that *N*-oxidation causes only a minor electronic directing effect toward this β,β'-addition reaction, whereby *N*-oxidation directs the dihydroxylation mildly away from the *N*-oxidized pyrrole moiety. This is an unexpected result as *N*-oxidation of, for instance, pyridine results in a dramatic electronic influence as expressed in the polarity inversion (Umpolung) reactivity of pyridine *N*-oxide.[21] On the other hand, we have previously pointed out that the UV−vis absorption spectrum of protonated *meso*-tetraphenylporphyrin and its *N*-oxide are identical, highlighting the minor electronic influence of the *N*-oxidation.[11]

The general stability and isolation of diolchlorin osmate esters is well documented.[22] The ^{1}H and ^{13}C NMR spectra of the diolchlorin osmate ester bispyridine adducts **2** and **3** indicate that they are both 2-fold symmetric (see spectra in the Supporting Information). Only one type of pyridine is visible. This suggests their cis-arrangement is anti to the cis-alkoxides, forming a N_2O_2 square plane around the Os(VI) center, further implying that the two oxo ligands complete the octahedral coordination sphere at the two axial positions. This is consistent with the findings of a range of crystallographically characterized osmate esters.[22]

Attempts to reductively cleave osmate ester **2** with H_2S were disappointing, and only a 23% yield of the desired diol **4** was isolated. The major product (60%) was the corresponding known deoxygenated tetraphenyl-2,3-diolchlorin.[16] The reduction of the osmate ester isomer **3** was slightly more successful (40% yield) but also produced the identical parent non-*N*-oxidized diolchlorin as the major product. Consistent with this implication of **4** and **5** being isomers of diochlorin *N*-oxide, their HR-MS (ESI+, 100% MeCN) are identical and conform with the expected composition ($C_{44}H_{33}N_4O_3$ for MH^+). Using *o*-phenylenediamine as a nonreductive reagent to cleave the osmate esters provided diolchlorin *N*-oxide isomers **4** and **5** in satisfactory yields (up to 70%) (Scheme 1).[23]

Spectroscopic Characterization of the Two Isomeric Diolchlorin *N*-Oxides. The UV−vis spectrum of **5** is identical to that of the known 2,3-dimethoxychlorin *N*-oxide,[11] strongly suggesting the presence of the *N*-oxide on the opposite side of the diolpyrrolidine moiety. Irrespective of this precedent, the ^{1}H NMR spectra of both **4** and **5** also allow the determination of their connectivity (Figure 1). The number of signals indicate the 2-fold symmetry of both isomers, thus excluding isomers that would place the pyrrolidine and oxygenated heterocycle next to each other. Diagnostic features suited to assigning the isomers are the relative shifts of the β- and pyrrolidine hydrogens, as compared to each other and to the corresponding signals of *meso*-tetraphenyl-2,3-dihydroxychlorin. The signals for isomer **5** are spread over a wider chemical shift range than those for isomer **4**. Considering only the signals for the two types of β-protons assigned to the pyrrole moieties flanking the diolpyrrolidines, they are spread 0.48 ppm in **5** but only 0.12 ppm in **4**. The greater chemical shift inequality for the β-protons in **5** can be interpreted as the effect of a modification of the molecule on two ends. Overall, the spectrum for **4** is similar compared to that of the parent diolchlorin, except for a 0.4 ppm

(15) (a) Brückner, C.; Sternberg, E. D.; MacAlpine, J. K.; Rettig, S. J.; Dolphin, D. *J. Am. Chem. Soc.* **1999**, *121*, 2609–2610. (b) Campbell, C. J.; Rusling, J. F.; Brückner, C. *J. Am. Chem. Soc.* **2000**, *122*, 6679–6685. (c) Daniell, H. W.; Brückner, C. *Angew. Chem., Int. Ed.* **2004**, *43*, 1688–1691. (d) McCarthy, J. R.; Hyland, M. A.; Brückner, C. *Org. Biomol. Chem.* **2004**, *2*, 1484–1491.

(16) Brückner, C.; Rettig, S. J.; Dolphin, D. *J. Org. Chem.* **1998**, *63*, 2094–2098.

(17) McCarthy, J. R.; Jenkins, H. A.; Brückner, C. *Org. Lett.* **2003**, *5*, 19–22.

(18) Lara, K. K.; Rinaldo, C. K.; Brückner, C. *Tetrahedron* **2005**, *61*, 2529–2539.

(19) Akhigbe, J.; Ryppa, C.; Zeller, M.; Brückner, C. *J. Org. Chem.* **2009**, *74*, 4927–4933.

(20) Ryppa, C.; Niedzwiedzki, D.; Morozowich, N. L.; Srikanth, R.; Zeller, M.; Frank, H. A.; Brückner, C. *Chem.—Eur. J.* **2009**, *15*, 5749–5762.

(21) Albini, A.; Pietra, S. *Heterocyclic N-Oxides*; CRC Press: Boca Raton, 1991; p 158.

(22) (a) Hawkins, J. M.; Meyer, A.; Lewis, T. A.; Loren, S.; Hollander, F. J. *Science* **1991**, *252*, 312–313. (b) Subbaraman, L. R.; Subbaraman, J.; Behrman, E. J. *Inorg. Chem.* **1972**, *11*, 2621–2627. (c) Wallis, J. M.; Kochi, J. K. *J. Am. Chem. Soc.* **1988**, *110*, 8207–8223. (d) Herrman, W. A.; Eder, S. J.; Scherer, W. *Chem. Ber.* **1993**, *126*, 39–43.

(23) We tested the cleavage/transamidation of the osmate ester with *o*-phenylenediamine on the parent osmate ester *meso*-tetraphenyl-2,3-diolchlorin osmate ester···$(pyridine)_2$, which gave us the corresponding known (ref 16) diolchlorin in 77% yield.

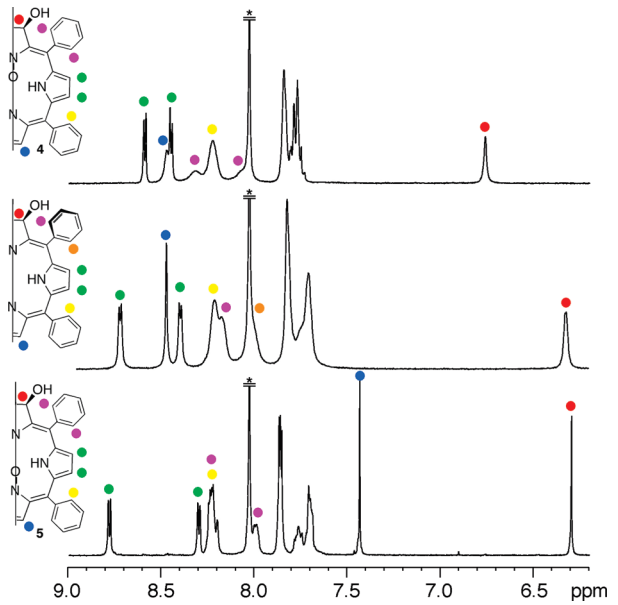

FIGURE 1. ^{1}H NMR (400 MHz, DMF-d_7, rt) spectral comparison of the aromatic region of **4** (top), *meso*-tetraphenyl-2,3-dihydroxychlorin (middle), and **5** (bottom). Unassigned peaks belong to the *m*-(higher-field region) and *p*-protons (lower field region) of the phenyl group.

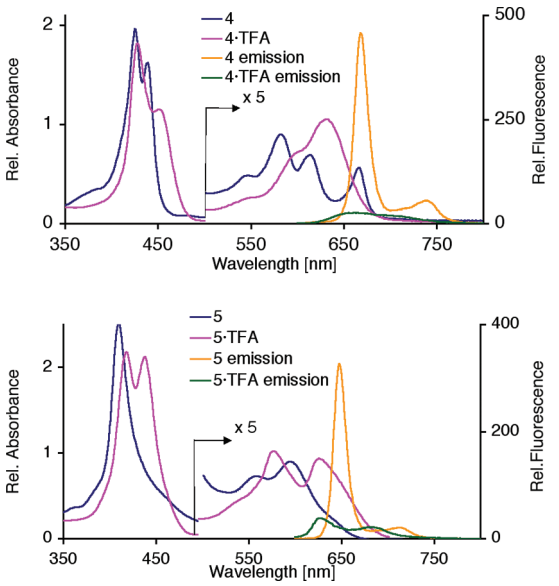

FIGURE 2. UV−vis absorption (blue trace, in CH_2Cl_2, and pink trace, in CH_2Cl_2 + 2% TFA) and fluorescence emission spectra [orange trace, in CH_2Cl_2, and green trace, in CH_2Cl_2 + 2% TFA; λ_{exc} at the isoabsorbance point, λ = 444 nm for **4** (top) and λ = 415 nm for **5** (bottom)]. The concentration of the chromophores in both solvents were (within 2% error) identical. Since the excitation wavelengths were selected to be the isoabsorbance point of the free base and acidified UV−vis spectra, the fluorescence intensities are directly comparable.

downfield shifted signal for the pyrrolidine hydrogen and a general 0.2−0.3 ppm high-field shift of all aromatic protons. On the contrary, the splitting pattern and relative shifts observed for **5** are different. A diagnostic example is the 1 ppm shift difference between singlets for the β-proton opposite of the diolpyrrolidine for **4** (s, 2H, 8.45 ppm) and **5** (s, 2H, 7.43 ppm) (cf. to s, 2H, 8.45 ppm for the parent diolchlorin). We have found previously that the signals for β-hydrogens of the pyrrole (or thiophene) moiety oxidized shift to high-field.[11] Thus, this assigns **5** to be the isomers with the *N*-oxide attached to the pyrrole opposite of the diolpyrrolidine.

The out-of-plane oxygens of *N*-oxide porphyrins and chlorins swing from one side of the plane of the chromophore through its center to the other side.[3,4] Thus, the two conformers one might expect for **5** are not found (cf. to the separation of the corresponding isomers in the dimethoxydithiachlorin *S*-oxide).[11] Likewise, no indication for the existence of separable conformers of **4** has been found.

Figure 2 shows a comparison of the UV−vis absorbance and fluorescence emission spectra of **4** and **5**. The free base UV−vis spectrum of diol **5** is analogous to that of *meso*-tetraphenylporphyrin *N*-oxide and, as expected, identical to that of known dimethoxychlorin *N*-oxide.[11,16] In general, the spectrum appears broadened; it likely reflects the dynamic process of the macrocycle and is not typical of a chlorin. Interestingly, the UV−vis spectrum of diol *N*-oxide isomer **4** is distinctly different from the spectrum of its regioisomer **5**; it features a split Soret band and greater number of (sharper) side bands but is also not chlorin-like. The longest wavelength of absorption (λ_{max}) for **4** is 665 nm, which is about 22 nm red-shifted compared to the parent diolchlorin. The finding that among a pair of *N*-oxide regioisomers, the isomer in which the β,β'-modified pyrrole moiety is *N*-oxidized is, compared to its isomer, bathochromically shifted can be generalized (see below). The fluorescence spectra are characterized by the small Stokes shift typical for porphyrins and chlorins. In both instances, the second vibronic band is clearly discernible.

The protonated spectra of *meso*-tetraarylporphyrin *N*-oxides were found to be near-identical to those of the protonated parent porphyrins.[11] The spectrum of **4** and **5** in CH_2Cl_2/2% TFA are vaguely similar to each other and to the protonated parent compound (split Soret, broadened side bands with sideband structures), though the Soret band of protonated **5** becomes overall more red-shifted. The fluorescence intensities of both **4** and **5** are, upon protonation, quenched by 80−90% of their free base values.

Chemical Reactivity of the Two Isomeric Diolchlorin *N*-Oxides 4 and 5 (and Their Osmate Esters 2 and 3). In order to evaluate whether the two isomeric diolchlorin *N*-oxides **4** and **5**, or the corresponding osmate esters **2** and **3**, showed any differential chemical reactivity, we subjected them to two oxidative functional group transformations. We, and others, established these transformations for the parent diolchlorins to lead to pyrrole-modified porphyrins (Scheme 1).[17,24,25]

Oxidation of *meso*-tetraaryl-2,3-dihydroxychlorin, or its osmate ester, with cetyltrimethylammonium permanganate (CTAP)[26] in CH_2Cl_2 generates cleanly the corresponding porpholactone.[17] Application of the CTAP reaction to osmate ester **3** or diol *N*-oxide **5** indeed furnishes porpholactone oxide **7** in good yields (71%). Compound **7** was

(24) Daniell, H. W.; Williams, S. C.; Jenkins, H. A.; Brückner, C. *Tetrahedron Lett.* **2003**, *44*, 4045–4049.
(25) Starnes, S. D.; Rudkevich, D. M.; Rebek, J., Jr. *J. Am. Chem. Soc.* **2001**, *123*, 4659–4669.
(26) (a) Bhushan, V.; Rathore, R.; Chandrasekaran, S. *Synthesis* **1984**, 431. (b) Furniss, B. S.; Hannaford, A. J.; Smith, P. G. W.; Tatchell, A. R. *Vogel's Texbook of Practical Organic Chemistry*, 5th ed.; Longman: Essex, 1989; p 549.

SCHEME 2. MTO/H_2O_2/Pyrazole Oxidation of TPP Dione 10

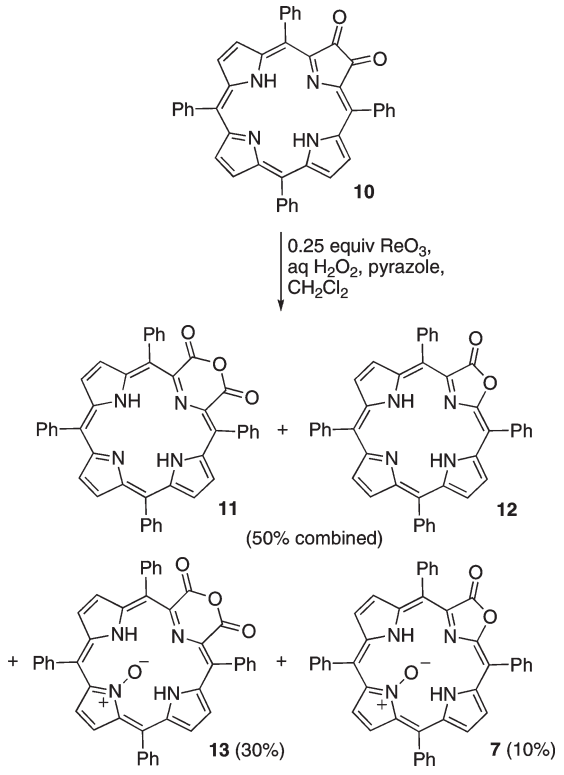

previously prepared by *N*-oxidation of porpholactone.[11] No intermediates are observed during these presumably multistep oxidations.

DDQ or periodinane oxidations of diolchlorins are known to generate the corresponding 2,3-diones.[24,25] Oxidation of diol **5** with Dess−Martin periodinane produces the corresponding *meso*-tetraphenyl-2,3-dione *N*-oxide **9** in 76% yield. The 2-fold symmetry of the product is reflected in its ^{1}H NMR spectrum that is also characterized by the absence of signals in the pyrrolidine hydrogen region. The presence of a carbonyl group is seen in the IR spectrum of **9** ($\nu_{C=O}$ = 1725 cm^{-1}), although this carbonyl group was undetectable in the ^{13}C NMR even when using delay times of up to 6 s and 10k scans (see the Supporting Information). The characteristic high-field shift of the β-pyrrole hydrogens of the *N*-oxidized pyrrole provide further indication for the location of the *N*-oxide. The formation of *meso*-tetraphenyl-2,3-dione *N*-oxide **9** is significant for two reasons. First, it provides an important clue to the mechanism of the formation of the porpholactone by oxidation of the diol (or its osmate ester) as oxidation of dione **9** with CTAP provides porpholactone **7**. In fact, the *m*-CPBA oxidation of a tetraphenylporphyrin-2,3-dione, reported by Crossley in 1984, was the first synthesis of a porpholactone.[27] Second, dione *N*-oxide **9** is not accessible through the direct MTO oxidation of *meso*-tetraphenylporphyrin-2,3-dione **10**. The outcome of the latter reaction is delineated below (Scheme 2).

An interesting gradation of the reactivity of the osmate ester **2** and diol *N*-oxide **4** under identical CTAP oxidation conditions is observed: Careful control of the reaction time

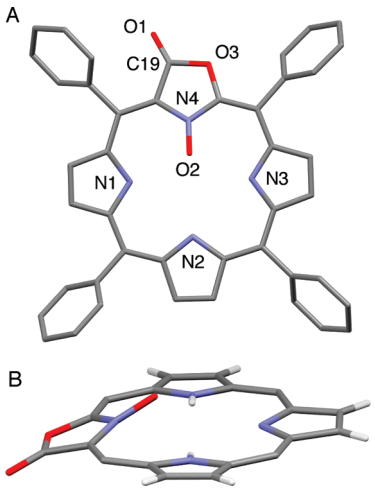

FIGURE 3. Stick representation of the single-crystal X-ray structure of **8**. (A) Top view: hydrogen atoms and disorder with respect to the relative orientation of the lactone moiety omitted for clarity. (B) Side view: phenyl groups and hydrogen atoms removed for clarity. Selected bond distances (Å): O2−N4, 1.337; C19−O1, 1.393; C19−O3, 1.195.

allows the isolation of dione **6** and lactone **8**, respectively, that both carry the *N*-oxide on the β,β'-modified pyrrole (Scheme 1). Evidently, the presence of the *N*-oxide moiety deactivates the oxidized pyrrole toward CTAP oxidations. The ^{1}H NMR and ^{13}C NMR spectra of both products allow their identification. In particular, the carbonyl group in **6** is at 176.7 ppm found 10 ppm upfield from that of the parent dione.[24,28] The carbonyl signal of **8** is also upfield shifted to 158.3 ppm (corresponding signal for the parent porpholactone at 167.3 ppm and for the *N*-oxide isomer **7** at 167.7 ppm).[11,29] Akin to the findings for the NMR-spectroscopic characterization of the diolchlorin *N*-oxide isomers **4** and **5**, the ^{1}H NMR spectra of the dione and porpholactone *N*-oxide isomers that carry the *N*-oxide on the pyrrole-modified unit (**6**, **8**) are much less spread compared to the spectra of their isomers (**7**, **9**). Porpholactone *N*-oxide **8** was also crystallographically characterized, removing all ambiguities in the assignment of all isomers.

Structural Characterization of Porpholactone *N*-Oxide 8. Porpholactone *N*-oxide isomer **8** provided crystals suitable for analysis by single-crystal X-ray diffractometry, the results of which are shown in Figure 3. This structure, the first of any pyrrole-modified porphyrin *N*-oxide, proves the spectroscopically derived connectivity and, in particular, the presence of the oxazolone *N*-oxide moiety. As was the case for tetraphenylporphyrin *N*-oxide,[11] the *N*-oxidized heterocycle is slanted out of the mean plane of the macrocycle and the macrocycle shows a minor waving distortion from planarity. However, the mean plane of the oxazolone is significantly more slanted (17.8°) with respect to the mean plane formed by the remaining non-hydrogen atoms of the macrocycle than the corresponding pyrrole *N*-oxide in *meso*-tetra(3,4,5-trimethoxyphenyl)porphyrin *N*-oxide (8.8°). In turn, the angle between the N4−O2 vector and the mean

(27) Crossley, M. J.; King, L. G. *J. Chem. Soc., Chem. Commun.* **1984**, 920–922.

(28) Crossley, M. J.; Burn, P. L.; Langford, S. J.; Pyke, S. M.; Stark, A. G. *J. Chem. Soc., Chem. Commun.* **1991**, 1567–1568.

(29) McCarthy, J. R.; Akhigbe, J.; Daddario, P.; Zeller, M.; Ranaghan, M. J.; Sandberg, M. N.; Birge, R. R.; Brückner, C. Manuscript in preparation.

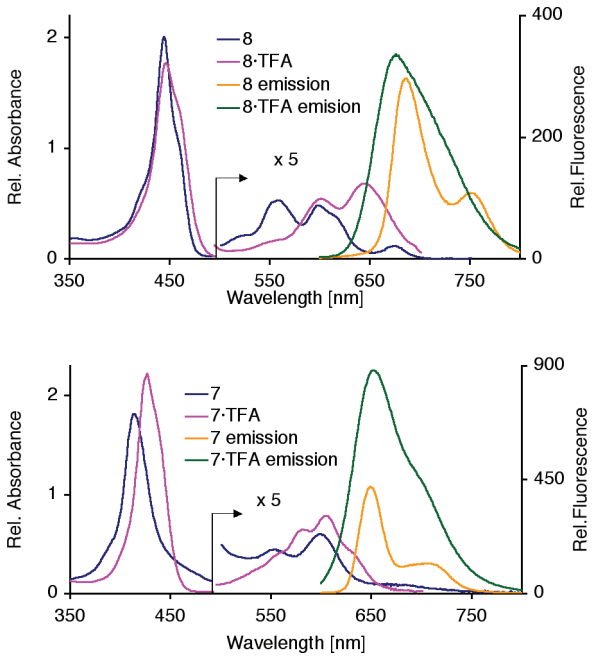

FIGURE 4. UV−vis absorption (blue trace, in CH_2Cl_2, and pink trace, in CH_2Cl_2 + 2% TFA) and fluorescence emission spectra [orange trace, in CH_2Cl_2, and green trace, in CH_2Cl_2 + 2% TFA; λ_{exc} at the isoabsorbance point of λ = 448 nm for **8** (top) and λ = 419 nm for **7** (bottom)]. The concentrations of the chromophores in both solvents were (within 2% error) identical. The excitation wavelengths were selected to be the isoabsorbance point of the free base and acidified UV−vis spectra; thus, the fluorescence intensities are directly comparable.

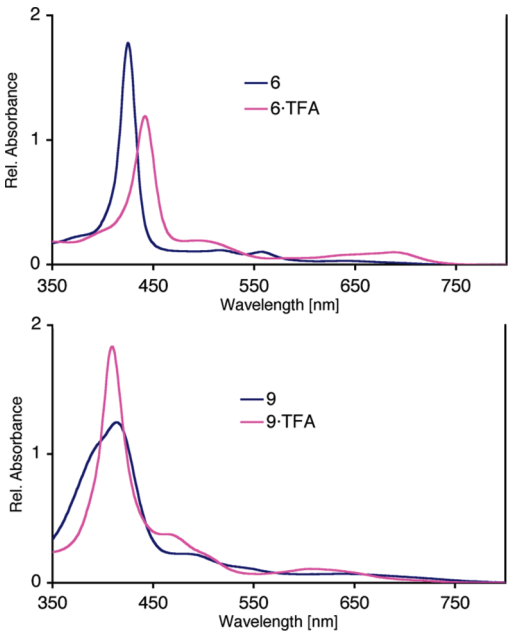

FIGURE 5. UV−vis absorption (blue trace, in CH_2Cl_2, and pink trace, in CH_2Cl_2 + 2% TFA) of **6** (top) and **9** (bottom). The concentrations of the chromophores in both solvents were (within 2% error) identical.

plane of the C_3O_2N oxazole moiety in **8** is opened from 131° in the porphyrin *N*-oxide to 167°. It is therefore closer to the linearity of the N−O bonds of, for example, pyridine *N*-oxides. The N4−O2 bond length is significantly longer (1.337(3) Å in **8** compared to 1.310(10) Å of the corresponding bond in *meso*-tetraarylporphyrin *N*-oxide).[11] The metric parameters of the lactone moiety and the remainder of the macrocycle are otherwise similar to those of known free base *meso*-tetraphenylporpholactone **12** (Scheme 2).[29]

Comparison of the Optical Properties of the Popholactone and Dioxochlorin *N*-Oxide Isomers. Figure 4 shows a comparison of the UV−vis and fluorescence spectra of **8** and **7**. The UV−vis spectrum for **7** under neutral conditions shows the typical pattern for *meso*-tetraphenylporphyrin *N*-oxide.[11] This is not surprising as the tetraphenylporphyrin and tetraphenylporpholactone possess very similar UV−vis and fluorescence spectra.[17,27,30] In comparison, the spectra for porpholactone *N*-oxide isomer **8** are distinctly different. The Soret band and λ_{max} are bathochromically shifted compared to the spectra for **7** and tetraphenylporpholactone. The UV−vis spectra of **7** and **8** in their acidified forms have a broad Soret band and the same number of side bands, though the spectrum of **8** is still more red-shifted. This shows that the electronic effect of *N*-oxidation is more clearly expressed when the *N*-oxidation has taken place on the pyrrole-modified moiety and much less so when it took place at a pyrrolic moiety. This compares to our earlier results that indicated the modest electronic influence of pyrrole *N*-oxidation.[11]

An unusual feature is notable in the porphyrin-type fluorescence spectra of **7** and **8**. Upon protonation of the macrocycle, the fluorescence is not quenched at all. It shows a slight increase for **8** and a significant increase for **7**. We cannot offer an explanation for the phenomenon, though we surmise it is an indication that the protonation events in **7**/**8** are significantly different from those of the other chromophores. Note that porpholactone *N*-oxide **8** possesses a considerable emission at 750 nm, an attractive range for molecular imaging applications of biological tissues.

Figure 5 shows a comparison of the UV−vis spectra of the dione *N*-oxide regioisomers **6** and **9**. The same trends delineated before are evident. The UV−vis spectrum of **9** is similar to the spectrum of the parent dione, and the pyrrole-2,3-dione *N*-oxide-containing isomer **6** is different and red-shifted. The same applies for the spectra of the protonated species. Compared to, for example, the diolchlorin *N*-oxides, the dione *N*-oxides fluoresce very dimly (not shown).

MTO/H_2O_2/Pyrazole Oxidation of *meso*-Tetraphenyl-2,3-dioxoporphyrin. The MTO/H_2O_2/pyrazole oxidation was well tolerated by a number of porphyrins and chlorins even though 2,3-diolchlorin decomposed.[11] When we attempted to convert 2,3-dioxochlorin **10** to the corresponding *N*-oxide **9**, we could not detect the formation of any trace of the expected dioxochlorin *N*-oxide **9**. Instead, four products were isolated in, depending on the reaction conditions (catalyst loading, time), varying amounts (Scheme 2). The products could invariably be distinguished as a pair of products formed early in the reaction, and a pair of products formed later in the reaction, and on the expense of the products formed initially. They were identified as anhydride **11** (early product, low polarity, brown), its corresponding *N*-oxide **13** (late product, high polarity, green), porpholactone

(30) Gouterman, M.; Hall, R. J.; Khalil, G.-E.; Martin, P. C.; Shankland, E. G.; Cerny, R. L. *J. Am. Chem. Soc.* **1989**, *111*, 3702–3707.

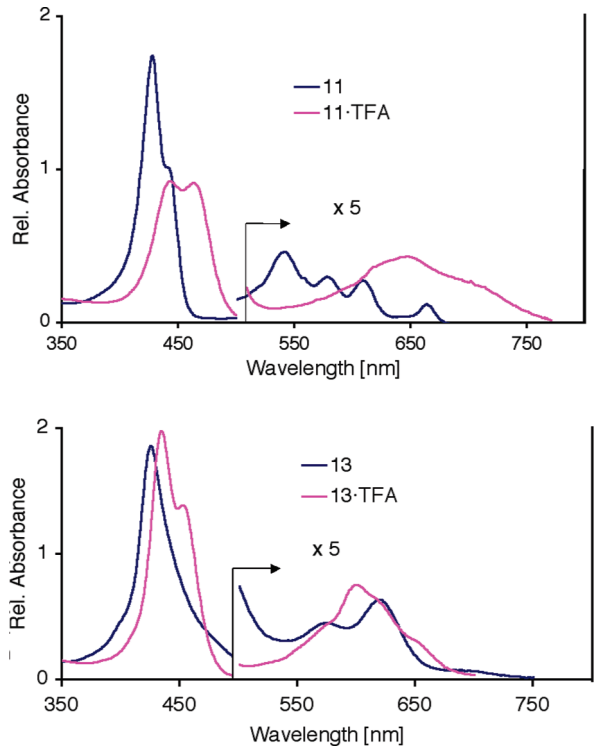

FIGURE 6. UV−vis absorption (blue trace, in CH_2Cl_2, and pink trace, in CH_2Cl_2 + 2% TFA) of **11** (top) and **13** (bottom). The concentrations of the chromophores in both solvents were (within 2% error) identical.

12 (early product, low polarity, purple), and its *N*-oxide **7** (late product, intermediate polarity, yellow-brown). Evidently, MTO/H_2O_2/pyrazole causes a Bayer−Villiger reaction on dione **10** to form the anhydride **11**. This reaction parallels a report by Crossley in which he used a peracid or air to convert dione **10** to **11**.[27] He further reported the fragmentation of **11** to form porpholactone **12**, a reaction we also observed. Consequently, *N*-oxides **13** and **7** are the expected products resulting from the MTO-catalyzed H_2O_2 oxidation of **11** and **12**, respectively. Reduction of the catalyst load (to 0.15 equiv) and short reaction times suppress the decarboxylation of **11**, and thus, anhydride **11** and its *N*-oxide **13** can be isolated in about 30% yields each. The ^{1}H NMR and ^{13}C NMR spectra of **13** confirm its 2-fold symmetry, and the characteristic shifts are observed to identify the position of the *N*-oxide.

Attempts to convert dione *N*-oxide **6** using an MTO-catalyzed oxidation to the corresponding anhydride *N*-oxide regioisomer of **13** failed. The reaction progressed very slowly and gave only trace amounts of porpholactone *N*-oxide **8** (Scheme 1).

Optical Properties of Anhydride 11 and Its *N*-Oxide. Figure 6 shows the UV−vis spectra of **11** and **13**. Considering the number and relative intensity of the side bands, the spectrum of anhydride **11** is a slightly red-shifted porphyrin spectrum. It is not chlorin-like, like the spectrum for morpholinochlorin .[17] It is thus another example to demonstrate the enormous influence of β-carbonyl groups on the porphyrinoid chromophore (porpholactone **12** and dione **10** are other examples).[31] The red-shift of **11**, particularly of its Soret band compared to that of porphyrins, may indicate the presence of a nonplanar macrocycle (structural information is not available for this chromophore). The spectrum of anhydride *N*-oxide **13** is reminiscent of the spectra of tetraphenylporphyrin *N*-oxide or porpholactone *N*-oxide **7**. The protonated spectra for **11** and **13** show similar features (split, red-shifted Soret, broad side bands), as discussed previously for the protonated spectra of porphyrins, porpholactones, and their *N*-oxides.

In summary, the MTO-mediated oxidation of porphyrins/chlorins and the OsO_4-mediated dihydroxylation of porphyrin *N*-oxides, combined with the manipulation of the resulting diol *N*-oxide isomers, are complementary to each other. These methods allow access to a number of isomeric chlorin-*N*-oxides. Thus, we have now access to four different *N*-oxide isomer pairs (**2** and **3**; **4** and **5**; **6** and **9**; **7** and **8**) of pyrrole-modified porphyrins for direct comparison. Generally, the isomers that contain the β,β'-bond modification and *N*-oxide group on the same heterocycle show larger electronic perturbations of their chromophores when compared to the isomers containing β,β'-modification and *N*-oxide on opposite sides of the macrocycle and the parent porphyrins/chlorins/pyrrole-modified porphyrins. Whether the novel chromophores possess properties that can be utilized for molecular imaging, sensing, or photomedical applications is a matter of current investigation.

Experimental Section

Materials and Instruments. All solvents and reagents were used as received. Analytical TLC plates: aluminum backed, silica gel 60, 250 μm thickness; preparative chromatography plates: 20 × 20 cm, glass backed, silica gel 60, 500, or 1000 μm thickness; flash column silica gel: standard grade, 60 Å, 32−63 μm. *meso*-Tetraphenylporphyrin *N*-oxide **1**[11] and *meso*-tetraphenyl-2,3-dione chlorin **10**[24] were prepared according to literature procedures.

***meso*-Tetraphenyl-2,3-*cis*-diolchlorin-24-*N*-Oxide Osmate Ester (2) and *meso*-Tetraphenyl-2,3-*cis*-diolchlorin-22-*N*-Oxide Osmate Ester (3).** In a 50 mL round-bottom flask equipped with a stirring bar was dissolved *meso*-tetraphenylporphyrin -oxide **1** (205 mg, 3.2×10^{-4} mol) in freshly distilled pyridine (20 mL) and the mixture treated with OsO_4 (3.2×10^{-4} mol, 1.62 mL of a stock solution of 500 mg of OsO_4 in 10 mL of pyridine). The flask was stoppered and stirred at rt for 5 days, all the while being shielded with aluminum foil. The disappearance of the starting material was followed by TLC and UV−vis spectroscopy. Once no further progress of the reaction was detectable, the solvent was removed in vacuo, and the residue was thoroughly dried under a gentle stream of N_2. The crude material was purified by preparative plate chromatography (silica−CH_2Cl_2/3% MeOH). The first low polarity fraction was starting material **1** (37% recovery). Compounds **2** and **3** were the second and third fractions.

2. Isolated in 25% yield. R_f (silica−CH_2Cl_2/3% MeOH) = 0.16. ^{1}H NMR (400 MHz, CD_2Cl_2/CH_2Cl_2, δ): 8.48 (d, ^3J = 4.6 Hz, 2H), 8.42 (s, 2H), 8.36 (brs, 4H), 8.29 (d, ^3J = 4.6 Hz, 2H), 8.17 (d, ^3J = 7.2 Hz, 2H), 8.12 (brs, 4H), 7.83 (d, ^3J = 7.2 Hz, 2H), 7.77 (m, 2H), 7.74−7.63 (m, 8H), 7.57 (d, ^3J = 7.4 Hz, 2H), 7.34−7.22 (m, 6H), 7.07 (s, 2H), 0.31 (brs, 2H). ^{13}C NMR 100 MHz, CD_2Cl_2/CH_2Cl_2, D1 = 3 s, δ): 150.1, 147.4, 142.9, 141.7, 140.5, 135.60, 135.55, 134.8, 134.6, 133.9, 133.3, 128.5, 128.1, 128.0, 127.7, 127.2, 127.15, 127.0, 126.4, 124.7, 113.9, 92.4. UV−vis (CH_2Cl_2) λ_{max} (nm) (rel intensity) 430 (1.00), 441 (sh),

(31) Brückner, C.; McCarthy, J. R.; Daniell, H. W.; Pendon, Z. D.; Ilagan, R. P.; Francis, T. M.; Ren, L.; Birge, R. R.; Frank, H. A. *Chem. Phys.* **2003**, *294*, 285–303.

540 (sh), 585(0.10), 614 (0.08), 667 (0.05). This osmate ester is not susceptible to analysis by ESI-MS.

3. Isolated in 35% yield. R_f (silica−CH_2Cl_2/3% MeOH) = 0.13. ^{1}H NMR (400 MHz, CD_2Cl_2, δ): 8.68 (d, ^3J = 4.6 Hz, 2H), 8.54 (d, ^3J = 7.3 Hz, 4H), 8.22 (d, ^3J = 4.6 Hz, 2H), 8.17 (brs, 4H), 7.98−7.94 (2 overlapping d, ^3J = 7.5 Hz, 4H), 7.80 (brs, 2H), 7.78−7.69 (m, 8H), 7.63 (t, ^3J=7.3 Hz, 2H), 7.56 (t, ^3J=7.3 Hz, 2H), 7.4−7.3 (m, 6H), 7.27 (t, ^3J = 7.3 Hz, 2H), 6.89 (s, 2H). ^{13}C NMR (100 MHz, CD_2Cl_2, D1 = 5 s, δ): 167.2, 150.1, 142.7, 142.5, 141.6, 139.6, 136.8, 135.8, 135.1, 132.7, 129.8, 128.6, 127.7, 127.53, 127.48, 127.2, 126.7, 121.2, 118.2, 116.6, 96.5, 71.1. UV−vis (CH_2Cl_2) λ_{max} (nm) (rel intensity) 414 (1.00), 549 (0.04), 598 (0.06). This osmate ester is not susceptible to analysis by ESI-MS.

***meso*-Tetraphenyl-2,3-*cis*-dihydroxychlorin 24-*N*-Oxide (4).** Method A: In a 20 mL scintillation vial with Teflon-lined cap and equipped with a stirring bar was dissolved green osmate ester **2** (20 mg, 1.9 × 10^{-5} mol) in CH_2Cl_2 (4 mL). *o*-Phenylenediamine (60 mg, 5.5 × 10^{-4} mol) was added and the mixture stirred at rt for 1 h. The solvent was evaporated, and the crude material was purified by preparative plate chromatography (silica−CH_2Cl_2/3% MeOH). Compound **4** was isolated in 37−70% yields as a dark green crystalline material by extraction of the silica gel with CH_2Cl_2/3% MeOH, followed by slow solvent exchange with petroleum ether 30−60 on the rotary evaporator. Method B: In a 25 mL round-bottom flask equipped with a stirring bar was dissolved osmate ester **2** (14 mg, 1.3 × 10^{-4} mol) in CH_2Cl_2 (5 mL) and MeOH (1 mL), and a stream of gaseous H_2S was passed through the solution for 1 min. The residue was filtered through a short plug of Celite (glass frit M), and the reaction mixture was dried under a stream of N_2. The crude material was purified by preparative plate chromatography (silica−CH_2Cl_2/3% MeOH). Compound **4** was isolated in 23% yield. R_f (silica−CH_2Cl_2/3% MeOH) = 0.17. ^{1}H NMR (400 MHz, 323K, DMF-d_7, δ): 8.57 (d, ^3J = 4.7 Hz, 2H), 8.45 (s, 2H), 8.42 (d, ^3J = 4.7 Hz, 2H), 8.25−8.15 (m, 8H), 7.84−7.70 (m, 12H), 6.70 (s, 2H), 0.37 (brs, 2H). OH protons could not be traced. ^{13}C NMR (100 MHz, 323 K, DMF-d_7, D1 = 3 s, δ): 155.2, 148.4, 143.1, 141.9, 141.1, 136.2, 135.2, 134.2, 129.1, 129.0, 128.8, 128.4, 128.0, 127.0, 125.0, 114.7, 71.1. UV−vis (CH_2Cl_2) λ_{max} (nm) (log ε): 425 (5.16), 438 (5.08), 540 (sh), 581 (4.12), 612 (4.01), 665 (3.92). UV−vis (CH_2Cl_2 + 2% TFA) λ_{max} (nm) (log ε): 428 (5.13), 450 (4.93), 538 (sh), 591 (sh), 632 (4.19). Fl (CH_2Cl_2, λ_{ex} = 444 nm): λ_{max} 668, 741 nm. Fl (CH_2Cl_2 + 2% TFA, λ_{ex} = 444 nm): λ_{max} 664 nm. HR-MS (ESI+, 100% CH_3CN): calcd for $C_{44}H_{33}N_4O_3$ (MH^+) 665.2553, found 665.2570.

***meso*-Tetraphenyl-2,3-*cis*-dihydroxychlorin 22-*N*-Oxide (5).** Compound **5** was prepared from osmate ester **3** (50 mg, 4.8 × 10^{-5} mol) according to the procedure described for **4**. Method A: 40% yield. Method B: 50% yield. R_f (silica−CH_2Cl_2/3% MeOH) = 0.21. ^{1}H NMR (400 MHz, DMF-d_7, δ): 8.78 (d, ^3J = 4.7 Hz, 2H), 8.30 (d, ^3J = 4.7 Hz, 2H), 8.26−8.19 (m, 6H), 8.01−7.98 (m, 2H), 7.89−7.83 (m, 6H), 7.8−7.74 (m, 2H), 7.74−7.64 (m, 4H), 7.43 (s, 2H), 6.3 (s, 2H). NH and OH protons could not be traced. ^{13}C NMR (100 MHz, DMF-d_7, D1 = 3 s, δ): 168.5, 143.1, 143.0, 141.7, 139.9, 137.2, 136.1, 135.5, 133.5, 130.7, 129.7, 128.6, 128.4, 128.2, 128.0, 122.0, 118.9, 117.4, 75.1. UV−vis (CH_2Cl_2) λ_{max} (nm) (log ε): 409 (5.22), 559 (4.08), 595 (4.16). UV−vis (CH_2Cl_2 + 2% TFA) λ_{max} (nm) (log ε): 418 (5.17), 437 (5.16), 576 (4.21), 626 (4.17). Fl (CH_2Cl_2, λ_{ex} = 415 nm): λ_{max} 649, 719 nm. Fl (CH_2Cl_2 + 2% TFA, λ_{ex} = 415 nm): λ_{max} 628, 687 nm. HR-MS (ESI+, 100% CH_3CN): calcd for $C_{44}H_{33}N_4O_3$ (MH^+) 665.2553, found 665.2570.

***meso*-Tetraphenyl-2,3-dioxochlorin 24-*N*-Oxide (6).** In a 20 mL scintillation vial with Teflon line cap and equipped with stirring bar was dissolved **2** (20 mg, 1.9 × 10^{-5} mol) in CH_2Cl_2 (4 mL). Cetyltrimethylammonium permanganate (CTAP) was added, and the reaction mixture was stirred at rt. The starting material was consumed after 1−2 h (by TLC) after which the reaction mixture was filtered through a short plug of Celite in a glass frit (M) and the solvent removed in vacuo. The crude brown residue was purified by preparative plate chromatography (silica−CH_2Cl_2). Product **6** was isolated in 56% yield as a brown powder by extraction of the silica gel with CH_2Cl_2 and solvent evaporation/exchange with petroleum ether 30−60. R_f (silica−CH_2Cl_2) = 0.4. ^{1}H NMR (400 MHz, CD_2Cl_2/CH_2Cl_2, δ): 8.79 (d, ^3J = 4.9 Hz, 2H), 8.71 (d, ^3J = 4.9, 2H), 8.62 (s, 2H), 8.16 (d, ^3J = 6.2 Hz, 4H), 8.09 (d, ^3J = 6.2 Hz, 4H), 7.83−7.74 (m, 12H), −1.8 (brs, 2H). ^{13}C NMR (100 MHz, CD_2Cl_2, D1 = 3 s, δ): 176.7, 157.9, 141.7, 139.7, 139.4, 138.3, 135.9, 135.0, 134.99, 130.8, 129.6, 129.1, 128.9, 128.7, 128.1, 127.5, 124.8, 115.0. UV−vis (CH_2Cl_2) λ_{max} (nm) (log ε): 425 (5.23), 514 (4.16), 558 (4.12), 600−700 (br sh). UV−vis (CH_2Cl_2 + 2% TFA) λ_{max} (nm) (log ε): 442 (5.06), 501 (5.33), 688 (4.11). HR-MS (ESI+, 100% CH_3CN): calcd for $C_{44}H_{29}N_4O_3$ (MH^+) 661.2240, found 661.2298.

***meso*-Tetraphenyl-2,3-dioxochlorin 22-*N*-Oxide (9).** In a 25 mL round-bottom flask equipped with a stirring bar was dissolved diol **5** (11 mg, 1.6 × 10^{-5} mol) in CH_2Cl_2 (4 mL). Dess−Martin periodinane reagent [1,1,1-tris(acetyloxy)-1,1-dihydro-1,2-benziodoxol-3-(1*H*)-one] (28 mg, 6.6 × 10^{-5} mol) was added, and the solution was stirred at rt for 24 h. The progress of the reaction was monitored by TLC. After all starting material was consumed, the solvent was removed in vacuo and the crude material purified by preparative plate chromatography (silica−CH_2Cl_2). Product **9** was isolated in 76% yield as a dark brown powder by extraction of the silica gel with CH_2Cl_2 and solvent exchange with petroleum ether 30−60. R_f (silica−CH_2Cl_2) = 0.2. ^{1}H NMR (400 MHz, CD_2Cl_2, δ): 8.85 (d, ^3J = 4.6 Hz, 2H), 8.45 (d, ^3J = 4.6 Hz, 2H), 8.18 (d, ^3J = 7.2 Hz, 4H), 7.89−7.71 (m, 12H), 7.67 (t, ^3J = 7.2 Hz, 4H), 7.52 (s, 2H). −NH not traced. ^{13}C NMR (100 MHz, CD_2Cl_2, D1 = 6 s, δ): 143.8, 141.9, 140.9, 140.6, 140.2, 138.6, 135.8, 133.5, 130.4, 130.3, 129.3, 128.4, 127.9, 127.6, 123.5, 120.9. UV−vis (CH_2Cl_2) λ_{max} [nm] (log ε): 394 (sh), 414 (5.08), 488 (4.39), 538 (sh), 600−800 (sh). UV−vis (CH_2Cl_2 + 2% TFA) λ_{max} [nm] (log ε): 409 (5.25), 469 (4.58), 609 (4.13). HR-MS (ESI+, 100% CH_3CN): calcd for $C_{44}H_{29}N_4O_3$ (MH^+) 661.2240, found 661.2289.

***meso*-Tetraphenyl-2-oxa-3-oxoporphyrin 24-*N*-Oxide (8).** Prepared from diol **4** (8 mg, 1.2 × 10^{-5} mol) according to the procedure described for synthesis of dione **6**. Product **8** was isolated in 35% yield as a deep green crystalline material. R_f (silica−CH_2Cl_2) = 0.69. ^{1}H NMR (400 MHz, CD_2Cl_2, δ): 8.79−8.77 (m, 3H), 8.70 (d, ^3J = 4.86 Hz, 1H), 8.58 (d, ^3J = 4.25 Hz, 1H), 8.54 (d, ^3J = 4.25 Hz, 1H), 8.16 (d, ^3J = 6.1 Hz, 8H), 7.83−7.76 (m 12H), 0.19 (brs, 2H). ^{13}C NMR (100 MHz, CD_2Cl_2, D1 = 3 s, δ): 158.3, 158.1, 156.8, 144.1, 141.7, 141.4, 139.9, 139.1, 139.0, 138.1, 137.2, 137.0, 135.9, 135.1, 134.7, 134.6, 134.53, 134.49, 130.7, 129.5, 128.94, 128.88, 128.3, 128.2, 128.1, 127.1, 127.0, 126.5, 125.3, 121.9, 119.4, 102.9. UV−vis (CH_2Cl_2) λ_{max} (nm) (log ε): 444 (5.12), 516 (sh), 559 (3.84), 598 (3.84), 674 (3.19). UV−vis (CH_2Cl_2 + 2% TFA) λ_{max} (nm) (log ε): 446 (5.06), 460 (sh), 601 (3.85), 642 (3.95). Fl (CH_2Cl_2, λ_{ex} = 448 nm): λ_{max} 687, 750 nm. Fl (CH_2Cl_2 + 2% TFA, λ_{ex} = 448 nm): λ_{max} 680 nm. HR-MS (ESI+, 100% CH_3CN): calcd for $C_{43}H_{29}N_4O_3$ (MH^+) 649.2240, found 649.2299.

***meso*-Tetraphenyl-2-oxa-3-oxoporphyrin 22-*N*-Oxide (7).** Prepared from osmate ester **3** (10 mg, 9.61 × 10^{-6} mol) in 71% yield according to the procedure described for synthesis of dione **6**; reaction time 2 h. Spectroscopic data matched with literature data.[11] Fl (CH_2Cl_2, λ_{ex} = 419 nm): λ_{max} 652, 719 nm. Fl (CH_2Cl_2 + 2% TFA, λ_{ex} = 419 nm): λ_{max} 655, 698 nm.

***meso*-Tetraphenyl-2a-oxa-2,3-dioxoporphyrin (11) and *meso*-Tetraphenyl-2a-oxa-2,3-dioxoporphyrin 22-*N*-Oxide (13).** In a 20 mL scintillation vial with Teflon-lined cap and stirring bar

was dissolved dione **10** (20 mg, 3.1×10^{-5} mol) in CH_2Cl_2 (8 mL). In a separate vial, $MeReO_3$ (1.14 mg, 4.58×10^{-6} mol) was suspended in CH_2Cl_2 (1 mL) and mixed with a 30% aq H_2O_2 solution (75 μL, $\sim 9.3 \times 10^{-4}$ mol) by vigorous shaking. This was added to the solution of **10**, followed immediately by pyrazole (4.22 mg, 6.2×10^{-5} mol). The reaction was stirred at rt for 15 h, checked by TLC, and worked up by addition of MnO_2 ($\sim$10 mg). The reaction mixture was filtered through a plug of cotton, and the solvent was removed in vacuo. The crude material was purified by preparative plate chromatography (silica$-CH_2Cl_2$). **11** was the low polarity first fraction, **13** the higher polarity second fraction.

11. Isolated in 39% yield as a green powder. R_f (silica$-CH_2Cl_2$) = 0.73. ^{1}H NMR (400 MHz, $CDCl_3$ δ): 8.68 (d, ^3J = 5.0 Hz, 2H), 8.55 (s, 2H), 8.42 (d, ^3J = 5.0 Hz, 2H), 8.12 (d, ^3J = 7.6 Hz, 4H), 8.03 (d, ^3J = 7.6 Hz, 4H), 7.79−7.68 (m, 12H), −1.42 (brs, 2H). ^{13}C NMR (100 MHz, $CDCl_3$, D1 = 6 s, δ): 162.7, 141.5, 140.11, 134.8, 134.6, 134.0, 129.2, 128.6, 128.5, 128.2, 127.6, 127.4, 126.1. UV−vis (CH_2Cl_2) λ_{max} (nm) (rel intensity): 428 (1.0), 442 (0.58), 542 (0.072), 578 (0.054), 609 (0.051), 664 (0.033). UV−vis (CH_2Cl_2 + 2% TFA) λ_{max} [nm] (rel intensity): 444 (1.0), 463 (0.98), 640 (0.125). MS (ESI+, 100% CH_3CN, 30 V cone voltage): m/z 661 (MH^+).

13. Isolated as a dark green powder in 29% yield. R_f (silica$-CH_2Cl_2$) = 0.37. ^{1}H NMR (400 MHz, CD_2Cl_2, δ): 8.86 (d, ^3J = 4.8 Hz, 2H), 8.48 (d, ^3J = 4.8 Hz, 2H), 8.22−8.19 (m, 4H), 8.12−8.09 (m, 4H), 7.84−7.78 (m, 6H), 7.76−7.70 (m, 6H), 7.58 (s, 2H), 1.95 (brs, 2H, exchangeable with D_2O). ^{13}C NMR (100 MHz, CD_2Cl_2, D1 = 3 s, δ): 163.1, 142.7, 142.2, 140.8, 140.2, 139.0, 138.7, 135.9, 134.9, 131.3, 130.8, 129.5, 128.8, 128.1, 127.9, 123.9, 121.9, 121.3. UV−vis (CH_2Cl_2) λ_{max} [nm] (log ε): 425 (5.2), 572 (3.89), 620 (4.03). UV−vis (CH_2Cl_2 + 2% TFA) λ_{max} (nm) (log ε): 435 (5.22), 45 (5.07), 600 (4.11), 666 (3.48). HR-MS (ESI+, 100% CH_3CN): calculd for $C_{44}H_{29}N_4O_4$ (MH^+) 677.2189, found 677.2205.

X-ray Single-Crystal Diffractometry of 8. All experimental details, including the CIF file, are provided in the Supporting Information.

Acknowledgment. This work was supported by the US National Science Foundation under Grant Nos. CHEM-0517782 and CCMI-0730826 (to C.B.). The diffractometer was funded by NSF Grant No. 0087210, by Ohio Board of Regents Grant No. CAP-491, and by YSU.

Note Added after ASAP Publication. Figures 2 and 4 were corrected on January 15, 2010.

Supporting Information Available: Copies of the ^{1}H, ^{13}C NMR, and FT-IR spectra of the novel compounds and experimental details to the crystal structure determination of **8**, including the CIF. This material is available free of charge via the Internet at http://pubs.acs.org.